Electronic and optical excitations in crystalline conjugated polymers

J.-W. van der Horst, P. A. Bobbert, and M. A. J. Michels
Polymer Physics Group, COBRA Research School & Dutch Polymer Institute, Department of Applied Physics, Eindhoven University of Technology, P.O. Box 513, NL-5600 MB Eindhoven, The Netherlands
(Received 4 February 2002; published 29 July 2002)

We calculate the electronic and optical excitations of crystalline polythiophene and polyphenylenevinylene, using the *GW* approximation for the electronic self-energy and including excitonic effects by solving the electron-hole Bethe-Salpeter equation. We compare with our earlier calculations on an isolated polythiophene chain and polymer chains embedded in a dielectric medium. Surprisingly, we find for the crystalline calculations optical gaps and exciton binding energies that are significantly smaller than present experimental values. We attribute the disagreement to the fact that the quantum-mechanical coherence between polymer chains, present in the calculations, is absent in most experimental situations. We discuss possible reasons for this absence. Our general conclusion is that the picture of a polymer chain in a dielectric medium is most appropriate in describing the present experimental data on electronic and optical excitations in conjugated polymers.

DOI: 10.1103/PhysRevB.66.035206 PACS number(s): 78.40.Me, 71.20.Rv, 42.70.Jk, 36.20.Kd

I. Introduction

Semiconducting conjugated organic polymers have received increasing interest in recent years, especially since the discovery of electroluminescence[1] of these materials. The charge carriers and excitations in these materials have been studied extensively both experimentally and theoretically, but many important fundamental issues still remain unresolved.[2] For instance, the magnitude of the exciton binding energy in these materials is still disputed.[3] This is a very important quantity, since in photovoltaic devices (solar cells) one would like to have a small binding energy, facilitating the fast separation of charges, while in electroluminescent devices such as light-emitting diodes a larger exciton binding energy, to increase the probability of fast (radiative) annihilation of electron-hole pairs, is desirable.

In conventional semiconductors, such as Si and GaAs, the optical excitations are well described in terms of very weakly bound electron-hole pairs (so-called Wannier excitons) with a binding energy of the order of 0.01 eV. In crystals made of small organic molecules such as anthracene, the exciton is essentially confined to a single molecule (Frenkel exciton), leading to a binding energy of the order of 1 eV. The question is where exactly conjugated polymers fit in between conventional semiconductors on the one hand and molecular crystals on the other.

Ab initio calculations on a variety of conjugated polymers, within the local-density approximation to density-functional theory (DFT-LDA), yield equilibrium structures in very good agreement with experiments.[4–7] Unfortunately, the one-particle energies resulting from DFT cannot be formally interpreted as excitation energies,[8] nor are excitonic effects taken into account in these calculations. Recently, Green's function methods for the first-principles description of the electronic (one-particle) *and* optical (two-particle) excitations of extended systems have been developed and applied to several systems.[9–11] In the meantime, these methods have been applied to the conjugated polymers polyacetylene,[12] polyphenylenevinylene[12] (PPV), and polythiophene[13,14] (PT). For these three polymers calculations for an isolated polymer chain were performed, leading to a good agreement for the excitation energy of the lowest optically active singlet exciton, but a very large binding energy for this exciton. For PPV and PT the binding energies were 0.9 and 1.9 eV, respectively, to be compared with the experimental values of 0.48 ± 0.14 eV (Ref. 15) and 0.6 eV,[16] respectively. We have demonstrated that by embedding a polythiophene chain in a medium with the appropriate frequency-dependent dielectric constants, the exciton binding energy is reduced to 0.76 eV,[13,14] while the optical gap remains virtually unaffected. A similar drastic reduction of the exciton binding energy by interchain screening effects was predicted earlier by Moore and Yaron[17] in polyacetylene, within the semiempirical Pariser-Parr-Pople theory. Simplified exciton calculations with an empirical dielectric constant $\epsilon = 3$ for the embedding medium, gave us an exciton binding energy of 0.61 eV for PT and 0.54 eV for PPV.[18] These simplified calculations were also performed for a number of other conjugated polymers and exciton binding energies were systematically found in the range 0.4–0.6 eV.[18] The reason for the reduction of the exciton binding energy compared to the isolated chain is that the polarization of neighboring chains leads to an additional, long-range screening of the Coulomb interaction. This screening also reduces the one-particle gap, and apparently by about the same amount. It is important to note that these calculations are still quasi-one-dimensional in the sense that the wave-function overlap between adjacent chains, and hence their quantum-mechanical coherence, is neglected.

In a very recent study,[19] the one-particle spectrum of crystalline polyacetylene was calculated. Wave-function overlap leads to level splittings of the order of 0.5 eV at several points in the Brillouin zone. The one-particle gap, however, was found to be almost the same as for the isolated chain (2.1 eV). No results were given for the two-particle spectrum of crystalline polyacetylene. In the present paper, we study the one-particle and two-particle excitations of PT and PPV in a crystalline geometry, replacing the effective dielectric environment in our previous calculations by the actual environment in the crystal. Furthermore, the crucial difference between the present calculations and our earlier work on

PT[13,14] is that in the present calculations we do allow for wave-function overlap between adjacent chains.

II. THEORY: THE QUASIPARTICLE AND BETHE-SALPETER EQUATIONS

We follow the calculational schemes as originally proposed by Hedin,[20] for one-particle excitations, and Sham and Rice[21] and Strinati,[22] for two-particle excitations. We briefly recapture these schemes here. Our numerical implementation has been outlined in our earlier publications.[13,14] We use the Car-Parrinello scheme[23] to obtain the DFT-LDA geometries of the single polymer chains and take the experimental crystal structures.[24,25] For PT this leads to an orthorhombic unit cell with $a=14.80$ (chain direction), $b=14.75$, and $c=10.45$ a.u. and a setting angle of 32° between the two chains in the cell. For PPV we have a monoclinic unit cell with $a=12.50$ (chain direction), $b=14.93$, $c=11.43$ a.u., a monoclinic angle of 123°, and a setting angle of 33°.

The quasiparticle (QP), or one-particle, energies $E_{n\mathbf{k}}$ and wave functions $\phi_{n\mathbf{k}}(\mathbf{r})$ are found by solving the quasiparticle equation, which reads, in atomic units,

$$\left[-\frac{\nabla^2}{2}+V_{\text{ion}}(\mathbf{r})+V_H(\mathbf{r})\right]\phi_{n\mathbf{k}}(\mathbf{r}) + \int d\mathbf{r}'\Sigma(\mathbf{r},\mathbf{r}',E_{n\mathbf{k}})\phi_{n\mathbf{k}}(\mathbf{r}')=E_{n\mathbf{k}}\phi_{n\mathbf{k}}(\mathbf{r}), \quad (1)$$

where $V_{\text{ion}}(\mathbf{r})$ is the potential of the atomic cores (which we replace by a pseudopotential[26]), $V_H(\mathbf{r})$ is the Hartree potential, and $\Sigma(\mathbf{r},\mathbf{r}',E_{n\mathbf{k}})$ the electronic self-energy. For this self-energy, we use the GW approximation[20]

$$\Sigma(\mathbf{r},\mathbf{r}',t)=iG(\mathbf{r},\mathbf{r}',t)W(\mathbf{r},\mathbf{r}',t). \quad (2)$$

Actually, we solve the quasiparticle equation, Eq. (1), in the basis of DFT-LDA wave functions $\psi_{l\mathbf{k}}(\mathbf{r})$, with energies $\epsilon_{l\mathbf{k}}$:

$$\epsilon_{l\mathbf{k}}c^n_{l\mathbf{k}}+\sum_{l'}[\Sigma_{ll'\mathbf{k}}(E_{n\mathbf{k}})-V^{xc}_{ll'\mathbf{k}}]c^n_{l'\mathbf{k}}=E_{n\mathbf{k}}c^n_{l\mathbf{k}}, \quad (3)$$

where $V^{xc}_{ll'\mathbf{k}}$ are the matrix elements of the DFT-LDA exchange-correlation potential. $c^n_{l\mathbf{k}}$ are the expansion coefficients of the QP wave functions:

$$\phi_{n\mathbf{k}}(\mathbf{r})=\sum_l c^n_{l\mathbf{k}}\psi_{l\mathbf{k}}(\mathbf{r}). \quad (4)$$

In our implementation,[13,14] based on the space- (imaginary-) time formulation of Rojas *et al.*,[27] we have a two-pole expression for the energy dependence of the matrix elements $\Sigma_{ll'\mathbf{k}}(E)$, so that we can easily solve Eq. (3) self-consistently for $E_{n\mathbf{k}}$. Furthermore, although usually it is sufficient to only calculate the diagonal matrix elements of $\Sigma_{ll'\mathbf{k}}(E)$, meaning that the QP and DFT-LDA wave functions are almost equal ($\phi_{n\mathbf{k}}\approx\psi_{n\mathbf{k}}$), we can also investigate the influence of nondiagonal matrix elements.

We follow the usual practice and take for G the DFT-LDA Green's function and calculate W within the random-phase approximation. Somewhat better QP energies are obtained when performing a second GW cycle in which the Green's function is constructed with the QP energies of the first GW cycle instead of the DFT-LDA energies[28] (taking the same W as in the first cycle). We follow this procedure and find increases of QP gaps of about 0.1 eV with respect to the first GW cycle.

The GW quasiparticle, or one-particle, energies and wave functions, together with the screened interaction W, are the input of the matrix formulation of the electron-hole Bethe-Salpeter equation[21,22]

$$[E_{c\mathbf{k}}-E_{v\mathbf{k}}]A^i_{cv\mathbf{k}}+\sum_{c'v'\mathbf{k}'}[2V^x_{cv\mathbf{k},c'v'\mathbf{k}}\delta_{s,0}-W_{cv\mathbf{k},c'v'\mathbf{k}}] \times A^i_{c'v'\mathbf{k}}=E^iA^i_{cv\mathbf{k}}, \quad (5)$$

where c and v label conduction and valence bands, respectively. This yields the two-particle excitation energies E^i and exciton binding energies E^i_b (from $E^i_b=E_g-E^i$, with E_g the QP gap). $A^i_{cv\mathbf{k}}$ are the expansion coefficients of the exciton wave function:

$$\chi_i(\mathbf{r}_e,\mathbf{r}_h)=\sum_{cv\mathbf{k}}A^i_{cv\mathbf{k}}\phi_{c\mathbf{k}}(\mathbf{r}_e)\phi^*_{v\mathbf{k}}(\mathbf{r}_h). \quad (6)$$

$W_{cv\mathbf{k},c'v'\mathbf{k}}$ are matrix elements of the screened Coulomb interaction W and $V^x_{cv\mathbf{k},c'v'\mathbf{k}}$ are exchange matrix elements of the bare Coulomb interaction V. The exchange matrix elements are only present for singlet ($s=0$) excitons. The matrix elements of W are taken at zero frequency, which turns out to be a good approximation.[29] Because the QP and DFT-LDA wave functions are almost equal we can use the latter to evaluate these matrix elements. The above expressions are valid for excitons with zero total momentum, which are the optically relevant ones, and to which we limit our discussion here.

In our calculations, we neglect lattice relaxations in excited states. For oligothiophenes, it was shown that the lattice relaxation accompanying an extra electron is at most 0.04 eV (Ref. 30) for large n, whereas that accompanying the lowest-lying triplet exciton is about 0.2 eV.[31] The lattice relaxational energy of the lowest-lying triplet exciton can be considered as an upper bound for that of the lowest-lying singlet exciton, because the size of the triplet exciton is smaller than that of the singlet exciton.

The cutoffs in our computations (number of plane waves, bands, and $\mathbf{k}$ points taken into account and parameters of the time/frequency grids) were determined such that the GW QP gaps are converged to within 0.05 eV and exciton energies to within 0.1 eV (our DFT-LDA energies were much more accurate). Energy differences between levels close in energy will have a higher accuracy and therefore we will present our results in the following section in eV with a precision of two decimal places.

III. Results

A. Polythiophene (PT)

The calculated GW QP band structure for crystalline PT is shown in Fig. 1. We will call this situation III. It is inter-

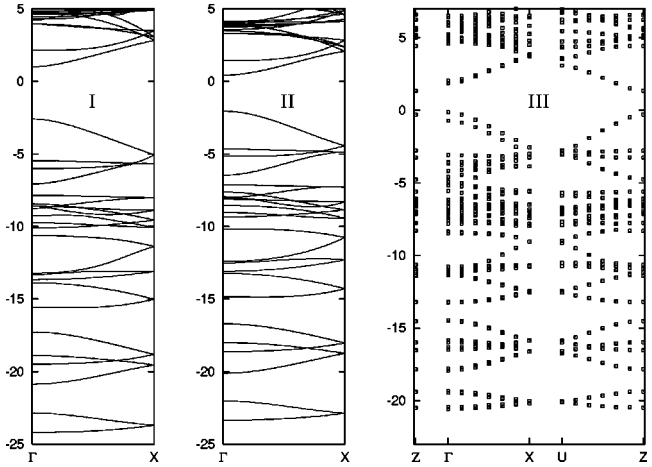

FIG. 1. The *GW* quasiparticle excitation energies (in eV) in polythiophene for situations I and II (isolated chain and chain embedded in dielectricum, from Refs. 13 and 14) and situation III (crystal, present work). Note that in situation III we have a double number of bands as compared to situations I and II, since there are two chains in the unit cell. In situation III we have an indirect gap of 1.48 eV between Γ and *Z*. In situations I and II the Brillouin zone is one dimensional and direct gaps of 3.58 and 2.49 eV, respectively, are found at Γ.

esting to compare this band structure with our earlier band structures for the single chain and for the chain embedded in a dielectric medium,[13] which we will call situations I and II, respectively. First of all, we have in situation III an *indirect* band gap of 1.48 eV between Γ and *Z*, whereas the gaps of 3.58 and 2.49 eV of situations I and II are direct. Second, the band structure along Γ-*X* in situation III, and in particular the behavior of the average of each split-up band, is very similar to situation II (and very dissimilar to situation I). To substantiate this, we have drawn in Fig. 2 a schematic diagram of the levels around the band gap for the three situations. We see that at Γ the splitting of in particular the top valence band is quite large, but that the *GW* band gap of 2.40

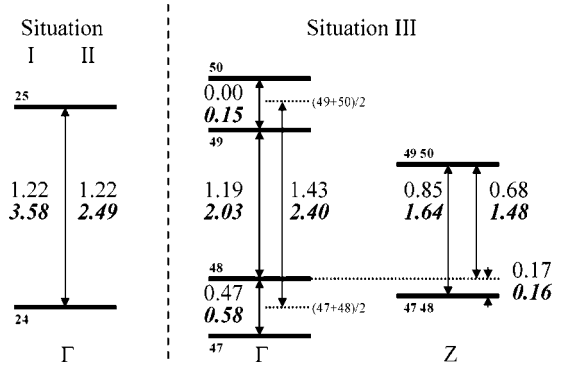

FIG. 2. Schematic diagram of the quasiparticle levels in polythiophene near the gap at Γ and *Z* (the latter for situation III only). All energies in eV, DFT-LDA in normal font, *GW* in bold italics. The small bold numbers near the levels are the band numbers. In situation III, the *GW* indirect gap of 1.48 eV occurs between Γ and *Z*. The experimental estimate for the one-particle band gap is 2.4–2.6 eV. (Refs. 32 and 16)

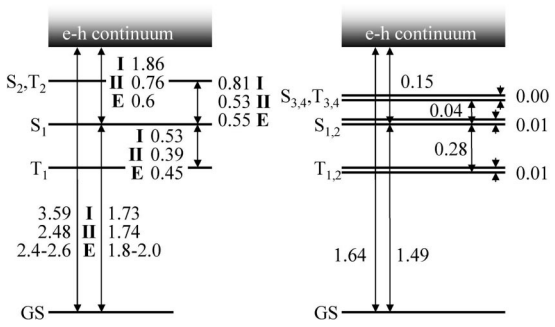

FIG. 3. The two-particle excitation energies (in eV) for the lowest few excitons in polythiophene for the situations I, II (from Refs. 13 and 14) and experiment (*E*, from Refs. 16 and 32) on the left, and in situation III (present work) on the right. In situation III, $S_{1,2}$ and $T_{1,2}$ are one-chain excitons, whereas $S_{3,4}$ and $T_{3,4}$ are off-chain excitons.

eV between the averaged top valence bands and bottom conduction bands is comparable to that of situation II (2.49 eV).

In Fig. 3 we have drawn a schematic level diagram of the lowest-lying excitons in PT, again for the three different situations. The optical matrix element of the S_1 exciton is by far the largest in all three situations. We already concluded in Refs. 13 and 14 that situation II yields results in good agreement with the experiments of Ref. 32. The optical gap of 1.49 eV in situation III is smaller than in situation II and too small in comparison with experiment. The reason for this is that the exciton wave function is mainly built up from products of conduction and valence states near *Z*, where the direct gap is smallest (1.64 eV), and considerably smaller than the direct gap of 2.49 eV at Γ in situation II (even lower-lying optically forbidden excitons with non zero total momentum will exist with wave functions built up from products of conduction states near *Z* and valence states near Γ). Additionally, we find in situation III small Davidov splittings of the exciton levels. The S_1 and S_2 excitons, e.g., correspond to symmetric and antisymmetric combinations of excitations on the two chains, respectively. It is interesting to note that the $S_{3,4}$ excitons are *off-chain*, or charge-transfer, excitons (electron and hole on different chains). Due to the smaller overlap between the electron and hole wave functions, the extra Coulomb energy needed to create such an exciton is almost compensated by the absence of the large positive exchange energy of the $S_{1,2}$ excitons, putting the $S_{3,4}$ excitons in energy just a little bit above the $S_{1,2}$ excitons. The very small exchange energy of these excitons also leads to a near degeneracy with the $T_{3,4}$ excitons.

The binding energy of the excitons in situation III should be defined with respect to the smallest direct gap (like in silicon), indicated by the ''electron-hole continuum'' in Fig. 3. Hence, we find a binding energy of 0.15 eV for the S_1 exciton, considerably smaller than the 0.76 eV found in situation II. Again, the reason for this is the dispersion of the bands perpendicular to the chains. The size of the S_1 exciton in situation III, however, is quite comparable to that in situation II and larger than in situation I, as can be seen in Fig. 4. We conclude from this that the dielectric properties in situations II and III, which determine the size of the excitons, are comparable.

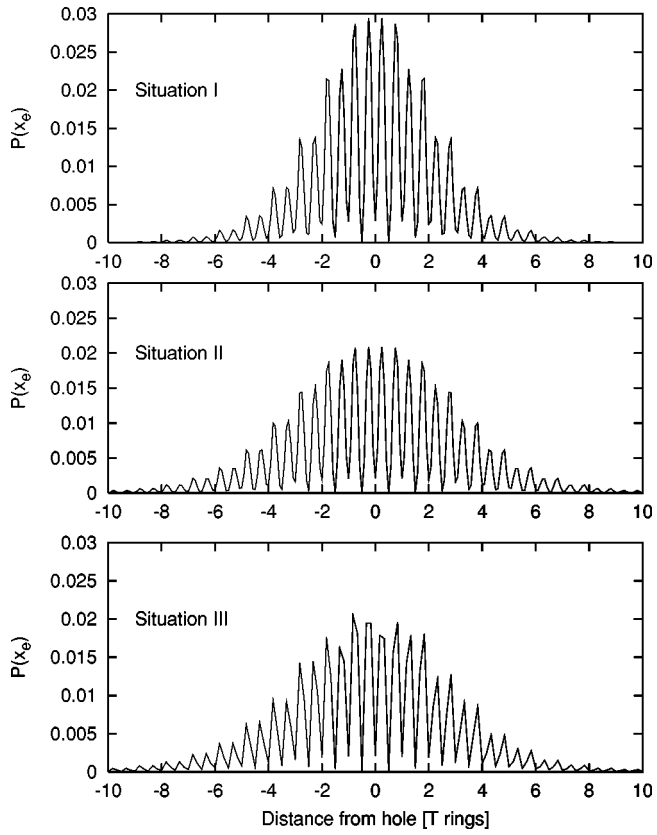

FIG. 4. The electron probability density (arbitrary units) along the polythiophene chain for the lowest optically active exciton S_1, for situation I (isolated chain), II (chain embedded in a dielectricum), and III (crystal). The position of the hole is kept fixed, at 1 a.u. above an inversion center. The distance is plotted in thiophene ring units of 7.4 a.u. The sizes of the excitons in situations II and III are comparable, indicating that the dielectric properties in these situations are similar.

B. Polyphenylenevinylene (PPV)

The calculated *GW* QP band structure for crystalline PPV is shown in Fig. 5. Contrary to PT, the band gap in the crystalline situation remains direct (as far as we can judge with our **k** sampling), with a gap of 2.10 eV at *B*. We have drawn a schematic level diagram for the points *A*, $(A+B)/2$ and *B* in Fig. 6. The point $(A+B)/2$ almost exactly corresponds to the point *X* in the one-dimensional band structure of a single PPV chain and the direction *A*-*B* is exactly perpendicular to the chain direction. The average gap at $(A+B)/2$ is 2.47 eV. With measured values of 2.4 eV (Ref. 33) for the optical gap and 0.48 ± 0.14 eV for the exciton binding energy,[15] the experimental fundamental gap of PPV would be about 0.4 eV larger than this value.

In Fig. 7 we have drawn a schematic level diagram of the lowest-lying four singlet and triplet excitons in PPV. The situation is now much more complicated than in PT. Because

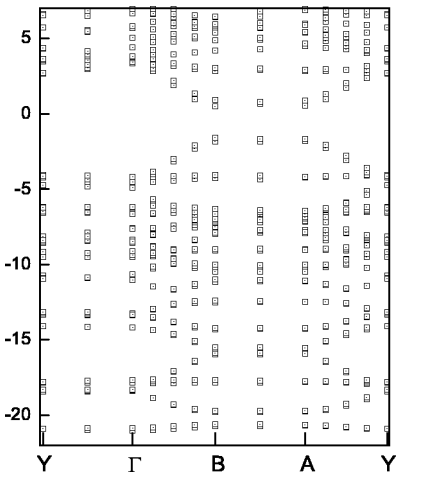

FIG. 5. The *GW* quasiparticle excitation energies (in eV) for crystalline PPV. The smallest direct gap of 2.10 eV is found at *B*.

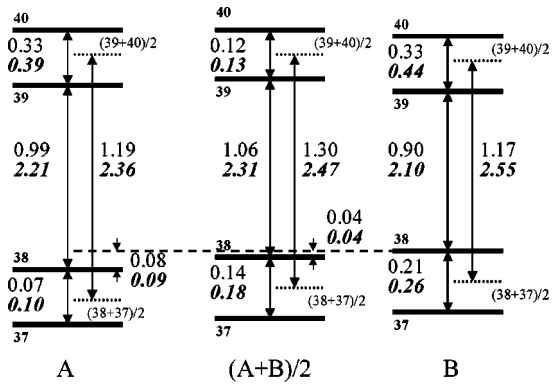

FIG. 6. Schematic diagram of the quasiparticle levels in crystalline PPV near the gap at *A*, *B*, and $(A+B)/2$. All energies are in eV, DFT-LDA in normal font, and *GW* in bold italics. The small bold numbers near the levels are the band numbers. The direct gap of 2.10 eV occurs at *B*. The experimental estimate for the gap is 2.9 eV (Refs. 15 and 33).

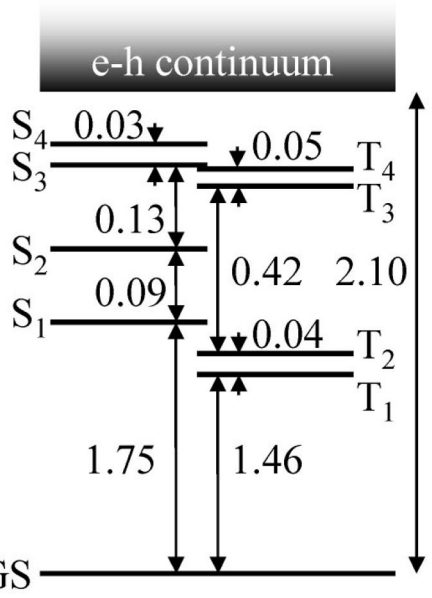

FIG. 7. The two-particle excitation energies (in eV) for the lowest few excitons in crystalline PPV. Due to the large hybridization, a clear separation into on-chain and off-chain excitons, like in PT (see Fig. 3), is not possible.

of the much larger splitting of the QP states involved in the exciton wave functions (the states near *A* and *B* in PPV, vs the states near *Z* in PT), a clear separation into on-chain and off-chain excitons and Davidov partners is no longer possible. The S_1, S_2, S_3, and S_4 excitons turn out to be built up mostly from products of states of bands 38 and 39 near *B*, 38 and 39 near *A*, 37 and 39 near *A*, and 37 and 39 near *B*, respectively. It is now the S_2 exciton that has by far the largest optical matrix element (S_1 and S_4 have small nonzero optical matrix elements). The predicted optical gap would be 1.75 eV (1.84 eV for the S_2 exciton) and the exciton binding energy is 0.35 eV (0.26 eV for the S_2 exciton), both smaller than the experimental values quoted above.

IV. DISCUSSION

The results of the preceding section, in combination with our earlier work,[13,14] inevitably lead to the conclusion that the inclusion of interchain screening effects is essential for a correct description of the electro-optical properties of conjugated polymers, but that the inclusion of interchain hybridization effects leads to serious disagreement with existing experimental data, at least for the important polymers polythiophene and polyphenylenevinylene.[34] There are two possible solutions to reconcile theory and experiment. Either the interchain hybridization is severely overestimated in our theoretical description, or it is somehow (almost) absent in present experiments. A reason why hybridization effects could possibly be overestimated is the use of the LDA, which is known to sometimes give unreliable results in situations where there are regions of low or rapidly varying electron density. Since the electron density in the region between the chains, which is the region that determines the hybridization, has this property, one can suspect the LDA to yield an erroneous hybridization. The *GW* and Bethe-Salpeter equation calculations based on LDA could inherit its errors. Therefore, we will investigate in the following corrections to LDA in the form of different gradient approximations, and in addition a truly nonlocal correction to LDA. The conclusion will be that the size of the hybridization predicted by LDA is correct. In the following sections we will then discuss possible reasons for the absence of hybridization in present experiments.

A. Overestimation of hybridization effects in LDA?

In LDA the long-range decay of the exchange-correlation potential is incorrect,[35] viz. exponential rather than the correct $1/r$ decay. Therefore, LDA puts too much charge in the outer regions. The effect is most pronounced in regions with the lowest charge density, in our case the regions between the chains. Surprisingly, gradient corrections to LDA do not correct this.[35] This means that part of the large hybridization (~ 0.5 eV) in the LDA may be an artifact of the method, rather than a real physical effect. In principle, this incorrectness of the LDA could be removed in a subsequent *GW* calculation. Nondiagonal matrix elements of the self-energy in the basis set of LDA wave functions could ''correct'' the LDA wave functions and decrease the hybridization. In a recent work of Grossman *et al.*[36] the LDA lowest unoccupied molecular orbital (LUMO) states of silane and methane were changed considerably by taking into account such nondiagonal matrix elements (apart from technical differences, the *GW*-BSE approach in that paper is the same as here). Taking all nondiagonal elements into account for the lowest 96 (48 valence and 48 conduction) bands in Eq. (3) in the case of PT did not significantly decrease the hybridization, however. Unfortunately, calculating all the nondiagonal elements for more bands was computationally not feasible. Mixing of higher conduction bands might therefore still reduce the hybridization.

TABLE I. Level splittings in eV due to hybridization of the isolated thiophene molecule C_4H_4S HOMO and LUMO states in the dimer $(C_4H_4S)_2$ at a molecule separation of 7.56 a.u. in two different orientations, calculated within DFT using five different potential and energy functionals.

		π stacked		Rotated and shifted	
Functional	Ref.	Δ_{HOMO}	Δ_{LUMO}	Δ_{HOMO}	Δ_{LUMO}
BLYP	38, 39	0.343	0.429	0.104	0.101
BP	38, 40	0.342	0.424	0.100	0.100
LB94	35	0.289	0.353	0.093	0.096
LDA	41	0.356	0.446	0.107	0.107
PW	42	0.340	0.428	0.105	0.108

In order to see if the hybridization of the wave functions in situation III is artificially large due to an error in the LDA, we performed a number of DFT calculations using various functionals as implemented in the ADF package.[37] In this package, the LB94 functional[35] is implemented. That functional was explicitly constructed to have a $1/r$ decay. Apart from this specific functional, more standard functionals, viz. Becke-Lee-Yang-Parr (BLYP),[38,39] Becke-Perdew (BP),[38,40] LDA (Ref. 41), (in a slightly different parametrization than the one used in in the main body of this work), and Perdew-Wang (PW) (Ref. 42) were also used for comparison. We performed calculations for the thiophene dimer, $(C_4H_4S)_2$, in two different geometries: π-stacked on top of each other, and rotated and shifted with respect to each other in such a way so as to represent the relative ordering of the rings in the PT crystal. The geometry of the isolated molecule was obtained within DFT-LDA and kept fixed for both geometries and all functionals. The results for the hybridization of highest occupied molecular orbital (HOMO) and LUMO states are given in Table I.

A number of interesting facts can be learned from Table I. First of all, LDA and most standard gradient corrections (BLYP, BP, and PW) give the same hybridization (within the accuracy of the method). Secondly, the LB94 potential, which has the correct behavior for long range and hence should be more reliable for weak, intermolecular interactions, give a hybridization that is only 15–25 % smaller than that of the other functionals. Note that the hybridization of the HOMO and LUMO for the shifted and rotated geometries (corresponding to the relative orientation of the rings of adjacent chains in our crystalline situation) is smaller by a

factor of 4 than the DFT-LDA predictions for situation III as given in Fig. 2. However, in this dimer configuration, each ring couples with only one other ring, whereas in the crystal there are six rings in the immediate surroundings of each ring, resulting in a larger hybridization than in the dimer studied here.

Even though the long-range behavior of the LDA is incorrect, which is believed to be troublesome for weak, intermolecular van der Waals interactions, the hybridization of the wave functions in LDA is not dramatically wrong. This is in line with LDA results for graphite, where good results for the interplanar distance were obtained,[43] for the binding distance and energy in the benzene dimer[44] and for the interchain distance for π-stacked polythiophene that we calculated. This strongly suggests that despite being formally incorrect for long-range interactions, LDA still gives reasonable results, and can therefore be relied upon to give a good estimate for the hybridization of the wave functions.

B. Side chains

Most experiments are performed on substituted polymers, i.e., some of the hydrogen atoms on the backbone or rings are replaced by large alkyl (θC_nH_{2n+1}) or alkoxy (θOC_nH_{2n+1}) side groups to improve the polymer's processability or other properties. These substituents dramatically alter the crystal structure from the crystal structure of the unsubstituted polymer. In particular, side chains will increase the distance between the main chains and therefore decrease the hybridization between the chains. We note that, because the interchain polarization between chains decays algebraically as a function of distance, whereas the wave-function overlap decays exponentially, the amount of interchain screening is not as much affected by the interchain distance as the interchain hybridization.

C. Static disorder

Polymers (substituted or unsubstituted) very rarely crystallize in a very orderly fashion. A sufficient amount of static disorder will prevent the occurrence of quantum-mechanical coherence between chains. In fact, it may be very difficult to reach conditions in which coherence occurs. In an experimental study of supposedly crystalline, unsubstituted PT, a density of $\rho = 1.21$ g/cm^3 was found.[45] For the crystal structure we have used for PT, $\rho = 1.54$ g/cm^3. If we assume the disorder in the size of the unit cell in the chain direction to be small (which is plausible since in that direction we have covalent bonds only), this means that the average interchain distances in the sample are $\approx 12\%$ larger than for the crystal structure we have used. Moreover, even in the ordered regions of the sample, the average displacement of the atoms from the perfect lattice sites is ≈ 0.3 Å.[45] Since the amount of wave-function overlap between two chains depends exponentially on the interchain distance, effective hybridization is practically impossible, even in more ordered samples.

This means that most experimental studies effectively look at isolated polymer chains in a dielectric medium, which is exactly what we studied for PT in situation II, the situation in which we have good agreement with present experimental data for the exciton binding energies, for various level splittings, and for the QP gap.

D. Dynamic disorder

In the case of oligomers, crystals of very high purity and crystallinity can be obtained. This means that for these systems, the assumed and experimental geometry are exactly the same and the wave-function hybridization and the resulting bandwidths can be expected to be of the same order as those predicted here, i.e., ~ 0.5 eV. However, a well-known effect in the oligomer crystals is the strong temperature dependence of the electron and hole mobilities.[46] Contrary to the situation in disordered systems, where charge transport is thermally activated, the mobility in these systems *decreases* when going from 0 to ~ 300 K, where a crossover to thermally activated behavior occurs for several oligomer crystals. The initial decrease is attributed to electron or hole mass renormalization, induced by thermally excited intermolecular phonon modes, which decreases the quantum-mechanical coherence between the chains. As most experiments are performed at 77 K or higher, interchain hybridization may be suppressed by this dynamic disorder even in perfectly crystalline polymers, leading to the same picture as sketched in the preceding paragraph, namely, that of an isolated chain in a dielectric medium.

V. SUMMARY AND CONCLUSIONS

We have calculated the quasiparticle band structure and lowest-lying exciton levels of crystalline polythiophene and polyphenylenevinylene, two very important conjugated polymers. Surprisingly, the obtained optical gaps and exciton binding energies are considerably lower than presently available experimental values. We attributed the disagreement to the quantum-mechanical coherence between the chains, present in the calculations, which causes considerable hybridization and shifts of energy levels. We excluded the possibility that this hybridization is an artifact of the approximations we use. This leads to the conclusion that effective hybridization between neighboring polymer chains is absent in most experimental situations. We have discussed three possible explanations for this absence: the presence of side chains, the presence of static disorder, and dynamic thermal disorder, destroying coherence even in perfectly crystalline systems. Therefore, the best description of the opto-electronic properties of the conjugated polymer systems investigated up to now is in terms of a single polymer chain embedded in a dielectric medium, the approach we followed in earlier works.[13,14,18] It remains an intriguing question whether the effects of hybridization predicted in the present work can be observed in very pure polymer crystals at low temperatures. A clue in this direction may be the recent scanning tunned microscope experiments on a ladder-type polyparaphenylene,[47] a polymer that, due to its stiffness, is very prone to crystal formation. Regions with different band gaps and exciton binding energies appear to exist in this

polymer: disordered regions with a relatively large (0.45–0.85 eV) and aggregate regions with a relatively small (~0.1 eV) exciton binding energy. This finding is qualitatively in line with the present work.

ACKNOWLEDGMENTS

We are grateful for many interesting discussions with Dr. S. F. Alvarado and Professor Dr. H. Bässler.

[1] J.H. Burroughes, D.D.C. Bradley, A.R. Brown, R.N. Marks, K. Mackay, R.H. Friend, P.L. Bum, and A.B. Holmes, Nature (London) **347**, 359 (1990).
[2] *Primary Photoexcitations in Conjugated Polymers*, edited by N.S. Sariciftci (World Scientific, Singapore, 1997).
[3] J.-L. Brédas, J. Cornil, and A.J. Heeger, Adv. Mater. **8**, 447 (1996).
[4] P. Vogl and D.K. Campbell, Phys. Rev. B **41**, 12 797 (1990).
[5] G. Brocks, P.J. Kelly, and R. Car, Synth. Met. **55-57**, 4243 (1993).
[6] P. Gomes da Costa, R.G. Dandrea, and E.M. Conwell, Phys. Rev. B **47**, 1800 (1993).
[7] C. Ambrosch-Draxl, J.A. Majewski, P. Vogl, and G. Leising, Phys. Rev. B **51**, 9668 (1995).
[8] R.W. Godby, M. Schlüter, and L.J. Sham, Phys. Rev. B **37**, 10 159 (1988).
[9] L.X. Benedict, E.L. Shirley, and R.B. Bohn, Phys. Rev. B **57**, R9385 (1998).
[10] S. Albrecht, L. Reining, R. Del Sole, and G. Onida, Phys. Rev. Lett. **80**, 4510 (1998).
[11] M. Rohlfing and S.G. Louie, Phys. Rev. Lett. **80**, 3320 (1998).
[12] M. Rohlfing and S.G. Louie, Phys. Rev. Lett. **82**, 1959 (1999).
[13] J.-W. van der Horst, P.A. Bobbert, M.A.J. Michels, G. Brocks, and P.J. Kelly, Phys. Rev. Lett. **83**, 4413 (1999).
[14] J.-W. van der Horst, P.A. Bobbert, P.H.L. de Jong, M.A.J. Michels, G. Brocks, and P.J. Kelly, Phys. Rev. B **61**, 15 817 (2000).
[15] L. Rossi, S.F. Alvarado, W. Riess, S. Schrader, D.G. Lidzey, and D.D.C. Bradley, Synth. Met. **111-112**, 527 (2000).
[16] M. Liess, S. Jeglinski, Z.V. Vardeny, M. Ozaki, K. Yoshino, Y. Ding, and T. Barton, Phys. Rev. B **56**, 15 712 (1997).
[17] E.E. Moore and D. Yaron, J. Chem. Phys. **109**, 6147 (1998).
[18] J.-W. van der Horst, P.A. Bobbert, M.A.J. Michels, and H. Bässler, J. Chem. Phys. **114**, 6950 (2001).
[19] M. Rohlfing, M.L. Tiago, and S.G. Louie, Synth. Met. **116**, 101 (2001).
[20] L. Hedin, Phys. Rev. **139**, A796 (1965).
[21] L. Sham and T.M. Rice, Phys. Rev. **144**, 708 (1966).
[22] G. Strinati, Phys. Rev. B **29**, 5718 (1984).
[23] R. Car and M. Parrinello, Phys. Rev. Lett. **55**, 2471 (1985). For the implementations used here see: R. Stumpf and M. Scheffler, Comput. Phys. Commun. **79**, 447 (1994); M. Bockstedte, A. Kley, J. Neugebauer, and M. Scheffler, *ibid.* **103**, 187 (1998).
[24] S. Brückner and W. Porzio, Makromol. Chem. **189**, 961 (1988).
[25] Z. Mo, K.-B. Lee, Y.B. Moon, M. Kobayashi, A.J. Heeger, and F. Wudl, Macromolecules **18**, 1972 (1985).
[26] N. Troullier and J.L. Martins, Phys. Rev. B **43**, 1993 (1991).
[27] H.N. Rojas, R.W. Godby, and R.J. Needs, Phys. Rev. Lett. **74**, 1827 (1995).
[28] M.S. Hybertsen and S.G. Louie, Phys. Rev. B **34**, 5390 (1986).
[29] M. Rohlfing and S.G. Louie, Phys. Rev. B **62**, 4927 (2000).
[30] G. Brocks, Synth. Met. **102**, 914 (1999).
[31] G. Brocks (private communication).
[32] K. Sakurai, H. Tachibana, N. Shiga, C. Terakura, M. Matsumoto, and Y. Tokura, Phys. Rev. B **56**, 9552 (1997).
[33] R. Kersting, B. Mollay, M. Rusch, J. Wenisch, G. Leising, and H.F. Kauffmann, J. Chem. Phys. **106**, 2850 (1997).
[34] Despite the large hybridization in crystalline polyacetylene, comparable to the hybridization we find here for polythiophene and polyphenylenevinylene, the *GW* band gap of this polymer in the crystal is found to be the same as for the isolated chain (Ref. 19). However, polyacetylene is in many respects an exceptional polymer.
[35] R. van Leeuwen and E.J. Baerends, Phys. Rev. A **49**, 2421 (1994).
[36] J.C. Grossman, M. Rohlfing, L. Mitas, S.G. Louie, and M.L. Cohen, Phys. Rev. Lett. **86**, 472 (2001).
[37] ADF version 2000.02 by SCM; E.J. Baerends, D.E. Ellis, and P. Ros, Chem. Phys. **2**, 41 (1973); L. Versluis and T. Ziegler, J. Chem. Phys. **88**, 322 (1988); G. te Velde and E.J. Baerends, J. Comput. Phys. **99**, 84 (1992); C. Fonseca Guerra, J.G. Snijders, G. te Velde, and E.J. Baerends, Theor. Chem. Acc. **99**, 391 (1998).
[38] A.D. Becke, J. Chem. Phys. **84**, 4524 (1986); *ibid.* **85**, 7184 (1986).
[39] C. Lee, W. Yang, and R.G. Parr, Phys. Rev. B **37**, 785 (1988).
[40] J.P. Perdew, Phys. Rev. B **33**, 8822 (1986).
[41] S.H. Vosko, L. Wilk, and M. Nusair, Can. J. Phys. **58**, 1200 (1980).
[42] J.P. Perdew and Y. Wang, Phys. Rev. B **33**, 8800 (1986).
[43] M.C. Schabel and J.L. Martins, Phys. Rev. B **46**, 7185 (1992).
[44] E.J. Meijer and M. Sprik, J. Chem. Phys. **105**, 8684 (1996).
[45] Z. Mo, K.-B. Lee, Y.B. Moon, M. Kobayashi, A.J. Heeger, and F. Wudl, Macromolecules **18**, 1972 (1985).
[46] J.H. Schön, S. Berg, Ch. Kloc, and B. Batlogg, Science **287**, 1022 (2000); J.H. Schön, Ch. Kloc, and B. Batlogg, Phys. Rev. Lett. **86**, 3843 (2001).
[47] S.F. Alvarado, S. Barth, H. Bässler, U. Scherf, J.-W. van der Horst, P.A. Bobbert, and M.A.J. Michels, Adv. Funct. Mat. **12**, 117 (2002).